

# Development of Fragility Curves for Multi-Span Reinforced Concrete Bridges

Vinita Saxena and George Deodatis  
*Dept. of Civil and Environmental Engineering,  
Princeton University, Princeton, NJ 08544*

Masanobu Shinozuka  
*Dept. of Civil and Environmental Engineering,  
University of Southern California, Los Angeles, CA 90089*

Maria Q. Feng  
*Dept. of Civil and Environmental Engineering,  
University of California, Irvine, CA 92697*

**ABSTRACT:** This paper studies the impact of stochastic spatial variability of seismic ground motion on the seismic response of long, multi-span, reinforced concrete bridges. The spatially varying ground motion time histories at the structural supports are generated to be compatible with prescribed response spectra at the supports of the bridge, and to reflect a prescribed coherence function, apparent velocity of wave propagation and duration of strong ground motion. The time histories are modeled as stochastic vector processes and are simulated using a variation of the spectral representation method. The effect of spatial variability of seismic ground motion on the bridge response is studied using fragility curves. Fragility curves are established for a representative bridge considering two types of asynchronous support excitation: 1) all structural supports on same local soil conditions, and 2) different structural supports on different local soil conditions. For comparison purposes, fragility curves are developed when the bridge is subjected to identical support ground motion. Monte Carlo simulations involving nonlinear dynamic analyses of the bridge are used in conjunction with a maximum likelihood approach to establish the fragility curves.

## 1 INTRODUCTION

The potentially detrimental effect of spatial variation of seismic ground motion on the response of elongated structures has been recognized for some time. This paper develops fragility curves for a multi-span concrete highway bridge for two cases of asynchronous support ground motion: all structural supports on same local soil conditions and different structural supports on different local soil conditions. For comparison purposes, fragility curves are also established for the case of identical support ground motion, an assumption commonly used by engineers in practice.

This study takes into account spatial variability effects due to loss of coherence, wave propagation and different local soil conditions, and estimates the response of the bridge structure to asynchronous input ground motions by performing nonlinear dynamic analyses. The spatially varying ground motion time histories at the bridge supports are generated using a recently developed variation of the spectral representation method.

The likelihood of structural damage due to different levels of seismic ground motion is usually expressed by a fragility curve. A fragility curve describes the damage probability corresponding to a specific damage state, for various levels of ground shaking. In this study, five different damage states are defined ranging from no structural damage to collapse. This paper follows a Monte Carlo simulation based approach suggested by Shinozuka (1998) to develop the fragility curves.

## 2 FRAGILITY ANALYSIS METHODOLOGY

### 2.1 Bridge Description

An actual twelve-span continuous reinforced concrete bridge is selected for this study (Santa Clara Bridge). The geometry and boundary conditions for this bridge are shown in Fig. 1. The overall length of the structure is 1640.5 ft, and each one of the eleven piers has a height of 39.35 ft.

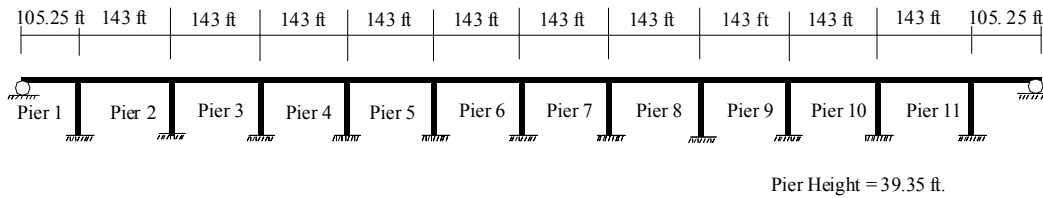
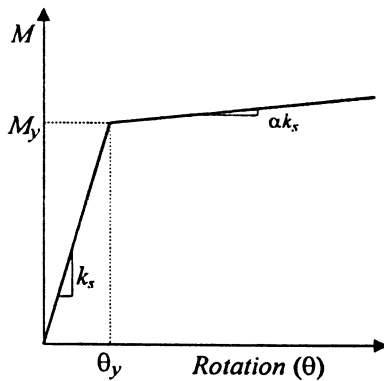
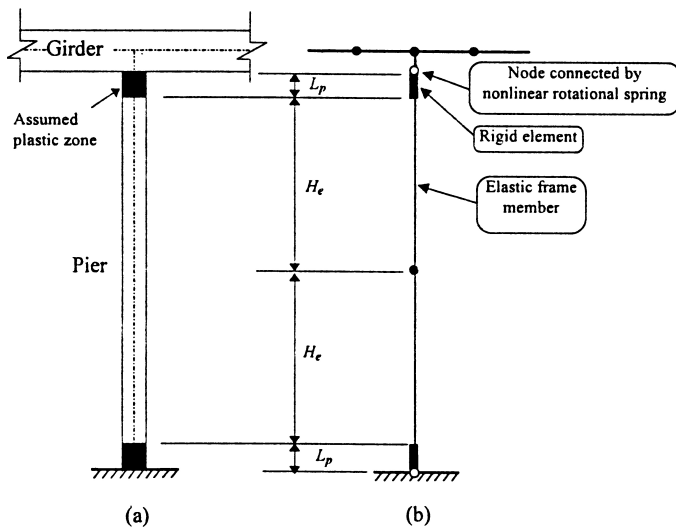


Figure 1. Santa Clara Bridge Configuration

## 2.2 Bridge Model

The bridge is analyzed with the SAP2000 finite element program (Computers and Structures 1998), using a two-dimensional finite element model consisting of a series of frame elements. The bases of the piers were assumed to be fixed, while the two abutments were modeled as roller supports.



(c)

Figure 2. Pier modeling by an elastic column and nonlinear rotational springs at both ends.

The model used to describe the potentially nonlinear behavior of the piers of the bridge (the only members considered to exhibit nonlinear behavior in this study) is depicted in Fig. 2a. According to this model, a pier is modeled as an elastic column of length  $2H_e$ , with a pair of plastic zones of length  $L_p$  at each end of the column, as shown in Fig. 2a. The total height  $H$  of the pier from the ground to the soffit of the girder is therefore equal to  $2(H_e + L_p)$ . Each plastic zone is then modeled to consist of a nonlinear rotational spring and a rigid element of length  $L_p$  as shown in Fig. 2b. The moment-rotation relationship used in this example for the nonlinear springs is the simple bilinear one shown in Fig. 2c. Its specific parameters are established using the *Column Ductility Program* COLx (Caltrans 1993) and detailed information of the cross-section of the pier. Fig. 2 is taken from Shinozuka et al. (1997). The parameter used to describe the (nonlinear) structural response is the *ductility demand*. This is defined as  $\theta/\theta_y$ , where  $\theta$  is the rotation of the nonlinear spring used to model the plastic zone at each end of a pier, and  $\theta_y$  is the corresponding yield rotation.

## 2.3 Simulation Algorithm and Ground Motion Characteristics

For this study, seismic ground motion time histories are generated at the supports of the bridge using a variation of the methodology suggested by Deodatis (1996).

At this point, a brief description of the original algorithm is provided. According to Deodatis (1996), the spectral representation method is used first to generate stationary ground motion time histories at the supports of the bridge that are compatible with a prescribed coherence function and a prescribed velocity of wave propagation, but not with the prescribed response spectra. These ground motion time histories are modeled as a stationary

stochastic vector process (with arbitrarily defined spectral density functions at the beginning of the iterative scheme involved in the methodology). After multiplying the generated stationary time histories by appropriate envelope functions to introduce non-stationarity, the resulting non-stationary time histories are used to compute the corresponding response spectra. These computed response spectra are then compared with the prescribed response spectra, and if they do not match, the diagonal terms of the cross-spectral density matrix of the underlying stationary stochastic vector process are upgraded according to the following formula:

$$S_i(\omega) \rightarrow S_i(\omega) \left[ \frac{RSA_i(\omega)}{RSA^{(i)}(\omega)} \right]^2 \quad (1)$$

where  $S_i(\omega)$  is the spectral density function of the  $i$ -th component of the stationary vector process,  $RSA_i(\omega)$  is the prescribed response spectrum for the  $i$ -th component, and  $RSA^{(i)}(\omega)$  is the computed response spectrum from the corresponding non-stationary time history of the  $i$ -th component.

The iterative scheme proceeds with the upgraded cross-spectral density matrix of the underlying stationary vector process, until the computed response spectra of the resulting non-stationary time histories match the corresponding prescribed response spectra with an acceptable level of accuracy. Such a convergence is achieved within a reasonable number of iterations (in most cases less than ten).

A recently recognized problem of the original algorithm described above, is that although at the end of the iterations the generated time histories closely reflect the prescribed response spectra, their coherence is generally somehow lower than the prescribed coherence. This is partly due to the fact that the upgrading of the spectral density functions according to Eq. (1) makes them eventually functions of the random phase angles used in the beginning of the iterative scheme to generate the first set of the underlying stationary time histories (refer to Deodatis 1996 for more details on the original algorithm). These random phase angles enter the spectral density functions through  $RSA^{(i)}(\omega)$ , the computed response spectra from the corresponding non-stationary time histories. The aforementioned problem arises because the amplitudes of the spectral density functions become random as the iterations proceed, and this violates one of the assumptions of the spectral representation algorithm (Shinozuka and Deodatis 1991). An additional complication of course is the nonstationarity of the generated time histories. The observed consequence is time histories (at the end of the iterative procedure) whose coherence is somehow lower than the prescribed coherence. It is

pointed out that it is rather important that the coherence of the simulated time histories be close to the target coherence, especially in the low frequency range, for the purposes of engineering applications.

In order to address this problem, the following two modifications are introduced to the original methodology: 1) Only sample functions that take a relatively small number of iterations to converge are kept. In this study, this number is set equal to four. 2) Smoothing the upgraded power spectral density functions by a simple rectangular window at each iteration. The modified iterative algorithm used in this study is shown in Table 1.

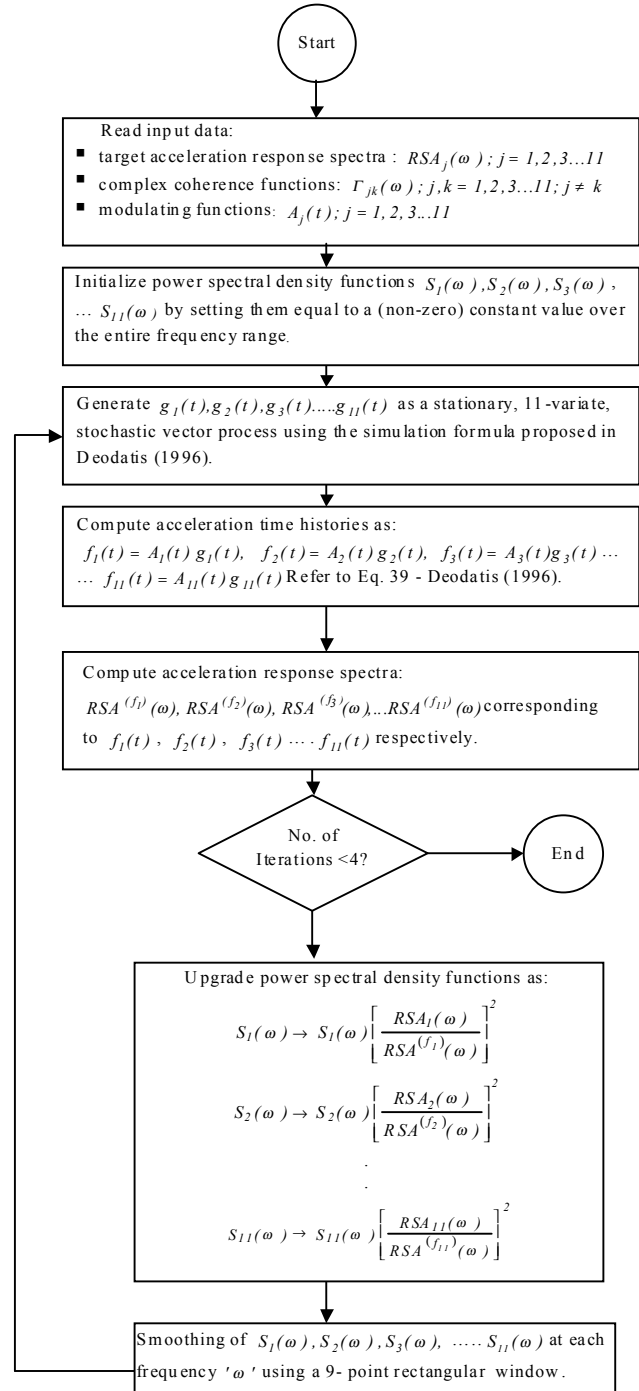


Table 1. Modified iterative procedure to generate response spectrum compatible acceleration time histories at eleven points on the ground surface.

Using the modified iterative procedure proposed in this study, the generated ground motion time histories at the end of the iterative scheme are not only compatible with the prescribed response spectra, but also accurately reflect the prescribed coherence function. In addition, a duration of strong ground motion can be specified through a modulating (envelope) function, and the simulated time histories reflect prescribed wave passage and loss of coherence effects. The local site effect is described by assigning different response spectra at bridge supports on different local soil conditions. The Uniform Building Code acceleration response spectrum for Type II soil is selected to describe the ground motion at piers on medium soil, and the UBC acceleration response spectrum for Type III soil is used to describe the ground motion at piers on soft soils. The Harichandran and Vanmarcke model (Harichandran and Vanmarcke 1986) is chosen to model the coherence loss between pairs of bridge supports.

The generated acceleration time histories are integrated to obtain the corresponding displacement time histories. For each set of differential (asynchronous) support ground motion time histories, the corresponding set of identical support time histories is obtained by considering that the displacement time history at the first support of the bridge is applied at all the other supports.

Several such sets of spatially varying ground motion time histories are generated at the bridge supports, and corresponding nonlinear dynamic time history analyses of the bridge are carried out along the lines of a Monte Carlo simulation procedure.

## 2.4 Damage States

Five different damage states are defined in terms of ductility demand of the piers, following the Dutta and Mander (2000) recommendations. They are displayed in the following table.

Table 2. Damage States

Damage State	Description	Ductility Demand
1. No Damage	First Yield ( $\sim\theta_y$ )	1.00
2. Slight Damage	Cracking, Spalling	2.01
3. Moderate Damage	Loss of Anchorage	6.03
4. Extensive Damage	Incipient Pier Collapse	11.07
5. Complete Collapse	Pier Collapse	23.65

## 2.5 Different Cases of Asynchronous Support Ground Motions Considered

In order to establish the fragility curves for the five different damage states defined above, the peak ground acceleration (PGA) is chosen to vary between 0.1g - 1.0g and a total 1,500 sets of ground motion time histories are generated in this range. The five cases of asynchronous support ground motion described in Table 3 are considered (for each one of these five cases, 1,500 sets of time histories are generated).

Table 3. Five Cases of Asynchronous Support Ground Motion Considered.

Case	UBC Soil Type II (Medium) at Piers	UBC Soil Type III (Soft) at Piers
1. DIFF	Pier 1-4, Pier 8-11	Pier 5-7
2. SAME-MEDIUM	Pier 1- 11	-
3. IDENT-MEDIUM	Ground Motion at Pier 1 applied at all the other piers.	-
4. SAME-SOFT	-	Pier 1- 11
5. IDENT-SOFT	-	Ground Motion at Pier 1 applied at all the other piers.

where:

i) DIFF - Different supports are on different local soils (with wave propagation velocity of 1000 m/s & loss of coherence according to the Harichandran-Vanmarcke model).

ii) SAME - All supports are on same local soils (with wave propagation velocity of 1000 m/s & loss of coherence according to the Harichandran-Vanmarcke model).

iii) IDENT - For each set of differential support ground motion time histories, the corresponding set of identical support ground motion time histories is obtained by considering that the ground motion time history at the first support is applied to all the other supports.

The five cases of asynchronous support ground motion defined in Table 3 are chosen for comparison with the standard assumption made in engineering design practice that all supports of the bridge experience identical support ground motions.

## 2.6 Fragility Curves

It is assumed that the fragility curves can be expressed in the form of two-parameter lognormal distribution functions. The estimation of these two parameters is done by the maximum likelihood method treating each event of bridge damage as a realization from a Bernoulli experiment (Shinozuka, 1998).

The likelihood function is expressed as (e.g. Shinozuka 1988):

$$M = \prod_{k=1}^N [F(a_k)]^{y_k} [1 - F(a_k)]^{1-y_k} \quad (2)$$

where  $F(\cdot)$  represents the fragility curve for a specific state of damage,  $a_k$  is the PGA value of the  $k$ -th set of acceleration time histories to which the bridge is subjected,  $y_k$  represents the realizations of the Bernoulli random variable  $Y_k$  with  $y_k = 1$  or 0 depending on whether or not the bridge sustains the specific state of damage under PGA equal to  $a_k$ , and  $N$  is the total number of sets of time histories for which the bridge is analyzed. Under the lognormal assumption,  $F(a)$  takes the following analytical form:

$$F(a) = \Phi \left[ \frac{\ln \left( \frac{a}{\alpha} \right)}{\beta} \right] \quad (3)$$

where  $a$  represents the PGA, and  $\Phi[\cdot]$  is the standardized normal distribution function. The two parameters  $\alpha$  and  $\beta$  (median and lognormal standard deviation) are computed in order to maximize  $\ln M$  (and hence  $M$ ) satisfying the equations:

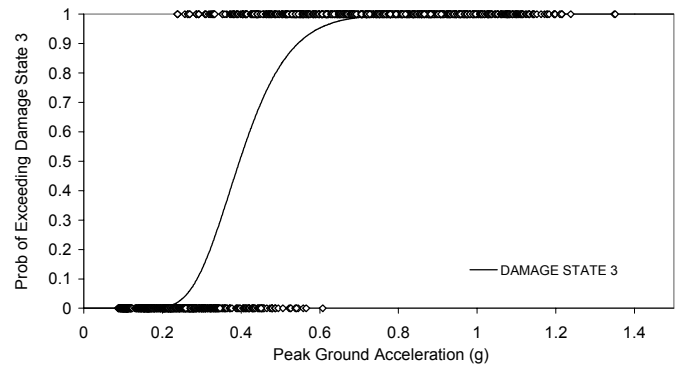
$$\frac{d \ln M}{d \alpha} = \frac{d \ln M}{d \beta} = 0 \quad (4)$$

This computation is performed numerically using a standard optimization algorithm.

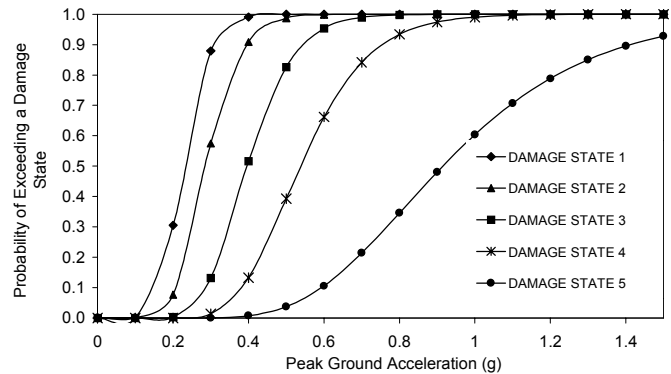
## 3 RESULTS AND CONCLUSIONS

Figure 3 displays the computed fragility curves for the Santa Clara Bridge. Figure 3a shows the

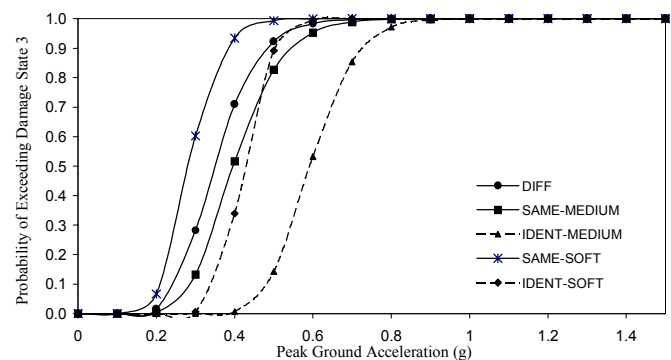
fragility curve associated with damage state 3 (moderate damage) and corresponding to Case 2 (SAME-MEDIUM). The diamonds plotted on the horizontal axis at the level of zero probability represent cases of time histories that produced ductility demands less than 6.03 (no moderate damage observed), while the diamonds plotted at the level of unit probability represent cases of time histories that produced ductility demands larger than 6.03 (moderate damage observed). The corresponding fragility curve computed according to these points (diamonds) is plotted with a continuous line in Fig. 3a. Figure 3b plots the fragility curves for all five different damage states for Case 2 (SAME-MEDIUM).



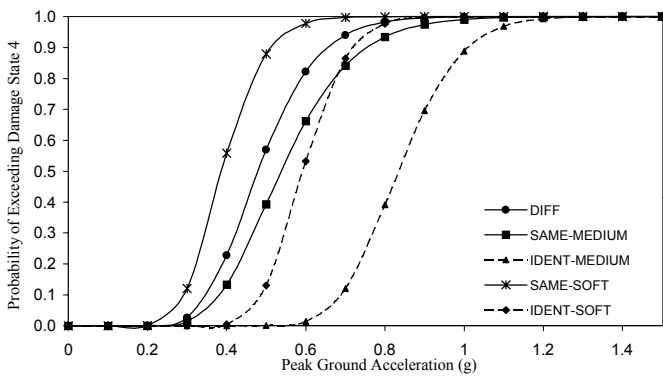
(a)



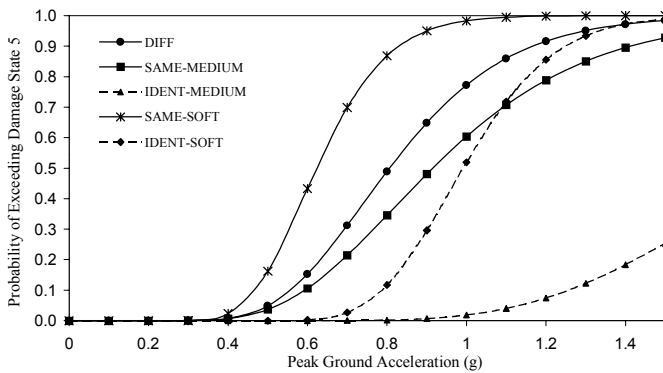
(b)



(c)



(d)



(e)

Figure 3: Fragility Curves for Pier 1 of the Santa Clara Bridge example.

The differences among the five cases of asynchronous support ground motion considered (i.e. DIFF, SAME-MEDIUM, IDENT-MEDIUM, SAME-SOFT, and IDENT-SOFT defined in Table 3) can be clearly observed in Figs. 3c (damage state 3 - moderate), 3d (damage state 4 - extensive) and 3e (damage state 5 - collapse). The fragility curves obtained in this study indicate that the bridge is more vulnerable to ground motion with spatial variation, compared to the corresponding case of identical support ground motion, for all levels of damage (refer to SAME-MEDIUM versus IDENT-MEDIUM and SAME-SOFT versus IDENT-SOFT curves in Figs. 3c, 3d, and 3e). In other words, the assumption of identical support ground motion is unconservative.

Under the assumption that Case 1 represents reality (bridge has supports on different local soil conditions), it becomes immediately obvious that any of the other four simplifying assumptions (of different levels of simplification of course), produces dramatically different probabilities of exceeding a certain level of damage.

It is concluded that it is of paramount importance to properly consider spatial variation of earthquake

ground motion for bridges similar to the one considered in this study. Further in-depth studies are needed to explore this issue for bridges of different spans and configurations, as it appears that it is not possible to generalize all conclusions drawn for the bridge examined in this study. In addition, fragility curves should also be developed using measures of ground motion intensity other than the PGA.

## ACKNOWLEDGEMENTS

The first two authors would like to acknowledge the support of the National Science Foundation under Grant No. CMS-95-23092 with Dr. Clifford J. Astill as Program Director.

The third author would like to acknowledge the support for this work of Multidisciplinary Center for Earthquake Engineering Research (MCEER)/NSF under Grant Number R98297 and MCEER/FHWA under Grant Number DTFH61-92-C00112 and DTFH61-92-C00106.

The fourth author would like to acknowledge the support of the National Science Foundation under Grant No. CMS-95-01796.

## REFERENCES

- California Department of Transportation - Division of Structures. (1993). "User's Manual for COLx, Column Ductility Program."
- Computers and Structures Inc. (1998). "SAP2000 Nonlinear Version 6.11 User's Reference Manual," Berkeley CA, 1998.
- Deodatis, G. (1996). "Non-Stationary Stochastic Vector Processes: Seismic Ground Motion Applications," *Probabilistic Engineering Mechanics*, Vol. 11, No. 3, pp. 149-167.
- Dutta, A. and Mander, J.B. (2000). "Seismic Vulnerability Analysis of Highway Bridges," *unpublished MCEER Technical Report*.
- Harichandran, R. S. and Vanmarcke, E. H. (1986), "Stochastic Variation of Earthquake Ground Motion in Space and Time," *Journal of Engineering Mechanics*, ASCE, Vol. 112, No. 2, pp.154-174.
- Shinozuka, M. (1998). "Statistical Analysis of Bridge Fragility Curves," *Proceedings of the US-Italy Workshop on Protective Systems for Bridges*, New York, N.Y., April 26-28.
- Shinozuka, M. and Deodatis, G. (1991). "Simulation of Stochastic Processes by Spectral Representation," *Applied Mechanics Reviews*, ASME, Vol. 44, No. 4, pp. 191-204.
- Shinozuka, M., Kim, J-M. and Purasinghe, R. (1997). "Use of Visco-Elastic Dampers at Expansion Joints to Suppress Seismic Vibration of Bridges," *Second National Seismic Conference on Bridges and Highways*, Sacramento, California, July 8-11.

